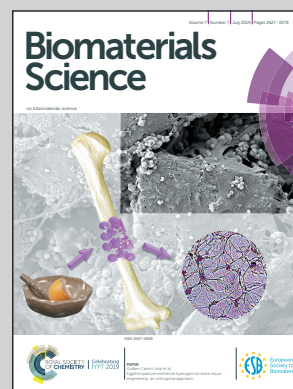**Highlighting research from the orthopedics department of Sun Yat-Sen Memorial Hospital, Sun Yat-Sen University.**

NOD2 negatively regulated titanium particle-induced osteolysis in mice

In contrast to traditional function of PRRs in inflammation, this article provides readers with new conclusion that NOD2 plays a negative role in osteolysis induced by titanium particles both *in vitro* and *in vivo*.

ROYAL SOCIETY OF CHEMISTRY | Celebrating IYPT 2019

rsc.li/biomaterials-science

Check for updates

NOD2 negatively regulated titanium particle-induced osteolysis in mice

Shixun Li,†[a] Junxiong Qiu,†[a] Ling Qin,[b] Peng Peng,[a] Changchuan Li,[a] Jiaji Mao,[c] Guibin Fang,[a] Zhong Chen,[a] Sipeng Lin,[a] Yuan Fu,[a] Weibin Cai*[d] and Yue Ding [ID] *[a]

For patients undergoing total joint replacement (TJR), one of the complications, aseptic loosening, could cause serious consequences, such as revision surgery. In early research, pattern recognition receptors (PRRs) were reported to play vital roles in recognizing wear particles from the prosthesis and initiating an inflammation response. In this research, we aimed to clarify the role of nucleotide-binding and oligomerization domain containing protein 2 (NOD2), one of the PRRs, in macrophage-induced aseptic loosening *in vivo* and *in vitro*. High expressions of NOD2 and TNFα were observed from twenty patients who underwent primary or revision total hip replacements (THR). The effect of NOD2 on the activation of inflammation pathways was observed in RAW264.7 cells and CRISPR-Cas9 NOD2-knockout mice. The expressions of NOD2, the NF-κB pathway, the MAPK pathway and proinflammatory cytokine TNF-α in macrophages stimulated by wear particles were up-regulated. Otherwise, inhibition of NOD2 further up-regulated the expressions of NOD2, the NF-κB pathway, the MAPK pathway and TNF-α. Knockdown of the NOD2 gene enhanced the cranial osteolysis induced by titanium particles in a mouse model. In conclusion, our study demonstrated that NOD2 plays a negative role in osteolysis induced by titanium particles *in vitro* and *in vivo*.

1. Introduction

TJR was one of the most revolutionary breakthroughs in orthopedic surgery due to its effect on pain release and long-lasting function of the reconstructed joint in the last century. It has been reported that 539 372 THRs were performed between 2003 and 2012 in England, Wales, and Northern Ireland.[1] In the United States, 2 552 815 individuals, 0.83% of the population, were living with hip prostheses in 2010.[2] However, for all the hip revisions from 2012 to 2017 in the United States, 12.0% of the patients were diagnosed as having aseptic loosening, which was one of the main causes for long-term revisions.[3] Therefore, research into the mechanism and prevention of hip aseptic loosening is critical for preventing the occurrence of aseptic loosening, lengthening the survival of the implants and could be helpful for the design of new prosthetic materials.

Previous studies have shown that wear particles from the prosthesis, inducing macrophage activation and finally leading to peri-prosthesis osteolysis, were the predominant cause of aseptic loosening.[4] It has been reported that sub-micron zirconium dioxide particles in a polymethylmethacrylate matrix released from bone cements were most abundant in tissue around cemented stems, while pure Ti and Ti alloy elements were mostly detected near uncemented cups. Polyethylene particles accounted for only a small part of the total number of particles around the prosthesis.[5] After interaction with wear particles, M0 macrophages turned into M1 macrophages and induced the secretion of proinflammatory cytokines, such as tumor necrosis factor-α (TNF-α), interleukin-6 (IL-6), interleukin-1β (IL-1β) and the receptor activator of nuclear factor-κB ligand (RANKL),[6] which could activate the osteoclasts and cause the peri-prosthesis osteolysis. The secretion of proinflammatory cytokine has been demonstrated to be adjusted by the size, shape and density of the wear particles in our studies.[7,8]

A large quantity of macrophages with a massive load of Toll-like receptors (TLRs) and nucleotide-binding and oligomerization domain-like receptors (NLRs) has been found in synovial membrane samples from aseptic loosening patients

[a]*Department of Orthopaedic Surgery, Sun Yat-Sen Memorial Hospital, Sun Yat-Sen University, Guangzhou 510120, China. E-mail: dingyue@mail.sysu.edu.cn*
[b]*Musculoskeletal Research Laboratory Department of Orthopaedics & Taumatology and Innovative Orthopaedic Biomaterial and Drug Translational Research Laboratory of Li Ka Shing Institute of Health Sciences, the Chinese University of Hong Kong, SAR, PR China*
[c]*Department of Radiology, Sun Yat-Sen Memorial Hospital, Sun Yat-Sen University, Guangzhou 510120, China*
[d]*Guangdong Engineering & Technology Research Center for Disease-Model Animals, Laboratory Animal Center and Department of Biochemistry, Zhongshan Medical School, Sun Yat-Sen University, Guangzhou 510080, China. E-mail: caiwb@mail.sysu.edu.cn*
† These authors contributed equally to this work.

in our previous studies,[9,10] indicating that macrophages might be able to recognize the wear particles through pattern recognition receptors (PRRs). In innate immunity, PRRs on the host cell surface or in the intracellular compartments recognize infections by detecting pathogen-associated molecular patterns (PAMPs) and some molecular structures exist only in pathogens.[11] But in recent studies, PRRs, especially TLRs, have been widely reported to recognize a variety of metals from the prosthesis, such as titanium particles, cobalt ions and CoCrMo implant particles and to respond by the activation of different inflammation pathways, and then cause the secretion of proinflammatory cytokines.[8,12,13] In our previous studies, we overexpressed the small heterodimer partner (SHP), an orphan nuclear receptor that negatively regulates the TLR4/NF-κB pathway and down-regulates the P65 expression of NF-κB. The expression of NF-κB was suppressed and the expression of proinflammatory cytokines was partly reduced.[8] Thus, we hypothesize that there might be other PRRs involved.

The NLRs are a large family of intracellular PRRs and consist of 23 members in humans and more than 34 members in mice. A domain structure including an intermediate nucleotide-binding (NBD or NACHT) domain, an N-terminal caspase recruitment domain (CARD) or a pyrin domain (PYD) and a C-terminal leucine-rich repeat (LRR) domain can be found in most of the members in this NLR family.[14] Based on their N-terminal domains or phylogenetics, NLRs are categorized into five subfamilies: NLRA, NLRB, NLRC, NLRX and inflammasome components.[15] NOD2 in the NLRC subfamily, containing two CARD domains, one NBD domain and one LRR domain, was the second member of the NLR family to be identified.[16] NOD2 is able to detect intracellular muramyl dipeptide (MDP) and can interact with the CARD-containing kinase RIP2 by ligand binding and activate the NF-κB pathway. Moreover, it can also signal induce the activation of MAPKs (p39, ERK and JNK) through the adaptor CARD9.[15] Activation of NF-κB and MAPK may lead to the inducement of transcriptional up-regulation of proinflammatory cytokines.

In this study, we aim to investigate the role of NOD2 in wear-particle-induced macrophage activation both *in vitro* and *in vivo*, and to seek for a potential target to treat aseptic loosening.

2. Materials and methods

2.1 Clinical specimen collection and immunohistochemistry assay

Clinical specimens were collected from 7 patients (3 males and 4 females, 15.090 ± 3.032 years after primary THA) who underwent revision surgery with the diagnosis of aseptic hip prosthesis loosening, and 13 patients (3 males and 10 females) who underwent primary THA with the diagnosis of femoral head necrosis (FHN), with an average age of 64.75 ± 8.50 years. Clinical specimens were collected from the synovial membrane around the prosthesis in the aseptic loosening group, and from hip synovial membrane in the FHN group.

All procedures were performed in accordance with the guidelines and approval of the Ethics Committee at Sun Yat-Sen University, Sun Yat-Sen Memorial Hospital ([2017] Ethic Record no. 26), and all patients were informed and agreed to this study.

Tissues were fixed in 4% formalin fixative and then embedded in paraffin blocks for 3.0 μm serial sectioning. The sections were then dehydrated using ethanol washes of increasing concentration, and deparaffinized using xylene. Endogenous biotin or enzymes were blocked with 3% hydrogen peroxide; antigen retrieval was treated with a high-pressure method. Anti-human CARD15 mouse monoclonal antibodies (1 : 100 diluted, Abcam, USA), anti-human TNF-α mouse monoclonal antibodies (1 : 100 diluted, Abcam, USA) and anti-human RANKL mouse monoclonal antibodies (1 : 100 diluted, Abcam, USA) were used as primary antibodies, and EnVision Detection Systems (DAKO, Denmark) were used as secondary antibodies. The tissues were incubated at 37 °C for 1 hour with primary antibodies, respectively, then washed with phosphate buffered saline (PBS) 3 times, and incubated at 37 °C for 0.5 hours with secondary antibodies. DAB was used as a chromogenic agent and hematoxylin was used for the second stain. Finally, the samples were washed with tap-water, dried, and mounted with neutral balsam, then observed by a biomicroscope (DM2000, Leica, Germany).

Ten views of each immunostained section were evaluated independently by two expert pathologists in a blind fashion. Bresalier's semiquantitative scoring system[17] was used, which evaluated both staining intensity (0 for no stain; 1 for weak stain; 2 for moderate stain; 3 for strong stain) and the percentage of stained cells. Scores for staining intensity and percentage positivity of cells from the two pathologists were then averaged and multiplied to generate the immunoreactivity score (IS) for each case: $\sum(0 \times F_0 + 1 \times F_1 + 2 \times F_2 + 3 \times F_3)$.

2.2 Particles

Titanium (Ti) particles (Alfa Aesar, Ward Hill, MA, USA) were diluted with pure water and then filtered by Isopore filter membranes (Millipore, MA, USA) in a filter holder, obtaining titanium particles of 0.2–1.2 μm, ending up with average diameters of 0.82 ± 0.12 μm.[8] These titanium particles were washed with 70% ethanol, then dried and weighed. Next, these particles were sterilized with ethylene oxide and then suspended in phosphate buffered saline (PBS), adjusting the concentration to $4 \times 10^8 \ mm^3 \ mL^{-1}$. The endotoxin level was undetectable (<0.01 EU per ml) in these particle suspensions *via* limulus amebocyte lysate assay (QCl-1000; BioWhittaker, Walkersville, MD, USA).[18]

2.3 Cell culture and particle stimulation

The macrophage cell line RAW264.7 (ATCC, Manassas, VA, USA) was cultured in DMEM medium supplemented (Gibco™ DMEM, Grand Island, NY) with 10% fetal bovine serum (FBS; Gibco) in a humidified incubator at a temperature of 37 °C with 5% CO₂. For analysis, cells were seeded in six-well tissue culture plates (Costar, Cambridge, MA, USA) with a quantity of

2×10^6 cells per well and then incubated overnight. Cell count and viability were assessed by a cell counter (Countstar BioTech), with viability exceeding 98% in all trials.

Twenty-four hours after the macrophages were seeded in the culture plates, titanium particles were added to each group. The particles were diluted to a final concentration of 100 : 1 (particle volume (cubic micrometers) : cell number) in the culture plates. Lipopolysaccharide (LPS) 100 ng L^{-1} and muramyl dipeptide (MDP) 1 μg ml^{-1} was used as a positive control and PBS was used as a negative control.[19] A highly potent and selective inhibitor of RIP2 kinase, GSK583 10 nM (MedchemExpress, USA) was used to block the NOD2-RIPK2 pathway.[20] Then, the culture plates were gently shaken for 5 minutes. After stimulation, the supernatants and RNAiso Plus (TaKaRa)-treated cells were harvested.

2.4 Flow cytometry

RAW264.7 cells were seeded onto 6-well plates at 5×10^5 cells per well. Macrophage bio-markers iNOS (M1) and CD206 (M2) were analyzed by flow cytometry to evaluate the different phenotypes. After 24 hours of culture, the cells were stimulated by titanium particles for 24 hours, then trypsinized, scraped from the plates, centrifuged, and resuspended in 1% bovine serum albumin (BSA) for 30 minutes at ambient temperature to block non-specific antigens. Then the cells were incubated with phycoerythrin (PE)-conjugated iNOS and allophycocyanin (APC)-conjugated CD206 for 30 minutes at ambient temperature. All antibodies used for flow cytometry were purchased from eBioscience. After washing twice with PBS, the cells were resuspended in 1% BSA and analyzed on a FACSVerse (Becton, Dickinson and Company, USA).

2.5 SiRNA synthesis and lentiviral transfection

Four siRNA sequences directed against the mouse NOD2 (Genbank accession no. AY160398.1) gene were designed and synthesized by GenePharma. Genome databases (BLAST, SSEARCH) were searched to ensure that these sequences would not target other mouse genes. A non-targeting siRNA was used as a negative control which would not target any known mouse gene, and an siRNA targeting mouse GAPDH (Genbank accession no. AY618199.1) was used as a positive control (Table 1). All of the siRNA sequences were labeled by FAM. Cells were cultured in serum-free OPTI-MEM medium (Invitrogen, Carlsbad, CA, USA) for one hour before transfection. RAW264.7 cells were transfected with 200 pmol of siRNA using 7.5 μl of Lipofectamine RNAiMate (Lipofectamine iMax Reagent, Invitrogen, USA) in each well. The medium was changed to DMEM with 10% FBS six hours after transfection. Transfection efficacy analysis was operated using fluorescence microscopy and flow cytometry 24 hours after transfection. Cells were harvested with RNAiso Plus, and the mRNA level of NOD2 was detected via real-time PCR to find the sequences yielding the greatest inhibition or over-expression effect of NOD2.

The recombinant lentivirus with the two sequences downregulating NOD2 was constructed by GenePharma. The lentivirus concentrated solution was obtained by screening positive clones and high-purity condensation, and the final titer was 8×10^8 TU per mL. A quantity of 2×10^5 cells per well was seeded in a six-well plate and then incubated overnight. Lentivirus, as mentioned before, was performed with 200 μl per well at a confluence of approximately 30%, according to the manufacturer's instructions, with a culture medium of DMED and 2 μg ml^{-1} polybrene for 24 h. The infected cells were then selected by fluorescent cell sorting. Transfection efficacy was 96.65% after fluorescent cell sorting.

2.6 Total RNA extraction and quantitative real-time PCR

Total RNA was extracted from the cells by using RNAiso Plus (TaKaRa, Dalian, PR China) the concentration of which was measured by NanoDrop technology (Thermo Scientific). Primescript RT MasterMix (TaKaRa, Dalian, PR China) was used to reversely transcribe the total RNA at the same concentration to cDNA following the manufacturer's instructions. The relative expressions of target genes were normalized using the housekeeping gene GAPDH. CFX Connect (Bio-Rad, USA) was used in quantitative real-time PCR to measure the mRNA levels. Data were calculated by the $2^{-\Delta\Delta CT}$ method. The primers of the target genes are shown in Table 2.

Table 1 Sequences of NOD2-siRNAs

Number	Gene	Gene sequence (5′ to 3′)
1	NOD2-689	CUCGCUUCCUCAGUACUUAUT UAAGUACUGAGGAAGCGAGTT
2	NOD2-1304	GCACAGAGUUGCAACUGAATT UUCAGUUGCAACUCUGUGCTT
3	NOD2-2443	GCUCUGUAUUUGCGAGAUATT UAUCUCGCAAAUACAGAGCTT
4	NOD2-2920	GGACUCAAGAGAAAUUCAATT UUGAAUUUCUCUUGAGUCCTT
5	Negative Control	UUCUCCGAACGUGUCACGUTT ACGUGACACGUUCGGAGAATT
6	GAPDH	CACUCAAGAUUGUCAGCAATT UUGCUGACAAUCUUGAGUGAG

Table 2 Primers of mRNAs used in this study

Gene	Forward	Reverse
NOD2	AGCACGTCAGGGAACTACCA	GGAAGCGAGACTGAGTCAACA
iNOS	GGAGTGACGGCAAACATGACT	TCGATGCACAACTGGGTGAAC
COX-2	TGCACTATGGTTACAAAAGCTGG	TCAGGAAGCTCCTTATTTCCCTT
IL-1β	GAAATGCCACCTTTTGACAGTG	TGGATGCTCTCATCAGGACAG
TNF-α	CCTGTAGCCCACGTCGTAG	GGGAGTAGACAAGGTACAACCC
GAPDH	TGTGTCCGTCGTGGATCTGA	TTGCTGTTGAAGTCGCAGGAG

2.7 TNF-α measurement by instant ELISA

At the time points 1 h, 2 h, and 4 h, cell supernatants were harvested and centrifuged to remove cellular debris. Then the excretive TNF-α were detected using a TNF-α instant enzyme-linked immunosorbent assay (ELISA) kit (eBioscience, Vienna, Austria), following the manufacturer's instructions.

2.8 Western blot

According to previous research, 1 hour was chosen as the time of stimulation for the MAPK pathway and the NF-κB pathway, and 4 hours was chosen as the time of stimulation for STAT1 to yield the most significant result.[21] After stimulation, the RAW264.7 cells with particles were lysed by RIPA buffer, protease and phosphatase inhibitors. Then the protein samples were fractionated by SDS-polyacrylamide gel electrophoresis using 10% polyacrylamide gel, electroblotted to polyvinylidene fluoride (PVDF) membranes. GAPDH was detected by GAPDH antibody (Abcam, 1 : 2000 dilution) as the protein loading control. Afterwards, the PVDF membranes were cut into small pieces according to different molecular masses, then incubated with primary antibody respectively and gently shaken overnight at 4 °C. Bound antibodies were then detected with a horseradish peroxidase-labeled secondary antibody (Abcam, 1 : 2000) and SuperSignal West Pico Chemiluminescent Substrate reagents (Pierce, Thermo Fisher Scientific, USA).

2.9 Immunofluorescent staining and confocal microscopy

RAW264.7 cells with or without transfection were respectively seeded at 0.4×10^6 cells per well in six well culture plates with three 1×1 cm pieces of glass in each well and incubated overnight. Two hours after stimulation (as mentioned before), the cells were washed 3 times with PBS and then fixed in 4% paraformaldehyde (PFA) for 15 minutes. Thereafter, the cells were treated with 0.1% Triton X-100 and gently shaken for 15 minutes for permeabilization, followed by three washes with PBS. Then the RAW264.7 cells were blocked in 1% bovine serum albumin (BSA) in PBS for 30 minutes, followed by incubation with 50 µl of primary antibodies diluted to 1 : 50 in 1% BSA in PBS overnight at 4 °C. The RAW264.7 cells were washed three times with PBS followed by incubation with secondary antibodies goat anti-rabbit IgG (H + L) labeled by red fluorescence (EarthOx Dylight 649) for 60 minutes. After washing three times with PBS, DAPI was added to the cells for nuclear counter-staining and they were mounted. Finally, the samples were imaged through a fluorescence microscope (Nikon) 24 h after mounting.

2.10 CRISPR-Cas9 NOD2-knockout mouse model

A mouse model with CRISPR-Cas9 NOD2-knockout mouse was developed in Guangdong Engineering & Technology Research Center for Disease-Model Animals. Briefly, the sequence of the sgRNA was determined using the CRISPR design web server by submitting the target sequence of the mouse NOD2 gene (GCTTGATCTCGCTGCGGTGA). A mixture of sgRNA and Cas9 protein was micro-injected into the cytoplasm of fertilized eggs obtained from mating between C57BL/6J males and superovulated females. The injected eggs were then transferred into the uterus of pseudopregnant C57BL/6J females. Genotyping of the founder mice was carried out by PCR amplification (caccgGCTTGATCTCGCTGCGGTGA) and direct gene sequencing. The selected founder mice were then mated with C57BL/6J mice, and heterozygous KI mice (F1) were identified and selected by both PCR amplification and direct gene sequencing. Homozygous mutant F2 offspring were bred from F1 heterozygous parents. Western blotting and direct gene sequencing using mouse tails was performed to confirm the NOD2-knockout. All the mice were fed to 25 weeks of age before surgery. Animal experiments were performed in accordance with the guidelines and approval of the Institutional Animal Care and Use Committee (IACUC) at Sun Yat-Sen University (L102022018060E).

2.11 Animal surgery

8-Week-old C57BL/6J male mice were purchased from the Animal Laboratory of Sun Yat-Sen University (Guangzhou, Guangdong, China). These animals were raised for 2 weeks in specific-pathogen-free conditions in the Laboratory Animal Center in Sun Yat-Sen University (Guangzhou, Guangdong, China), and so all mice were 10 weeks of age at surgery.

The WT mice and the NOD2-knockout mice were anesthetized by 10% chloral hydrate via intraperitoneal injection. A 15 mm midline sagittal incision on the head of the mouse was made for exposure of the calvaria. A 0.5×0.5 cm^2 gelatin sponge was placed under the periosteum over the calvaria. Titanium particles, lentiviral vector, MDP or GSK583 were injected respectively at the mid-line sagittal of the calvaria before suture. A sham operation (making a midline sagittal incision over the calvaria and suturing without injection) was taken as the blank control. Mice injected with PBS were used as a negative control group. No deaths or complications were observed during the 14 days' observation after the operation. Then, the mice were euthanized, and their calvaria were harvested with all soft tissues obliterated for micro-CT imaging.

The WT mice were divided into 9 groups, with 5 mice in each group. 30 µl of PBS containing 0.3 mg of titanium particles was locally injected into the Ti group, the Ti + NC-LV group and the Ti + NOD2-LV group. 70 µl of the NOD2 down-regulation shRNA lentiviral vector or negative control lentiviral vector with a titer of 8×10^8 TU per mL was locally injected into the Ti + NOD2-LV, Ti + NC-LV, NOD2-LV and NC-LV groups. The volume of the injection was adjusted to 100 µl by PBS. 100 µl of PBS was used as a blank control. In addition, after the titanium particles were locally injected, 40 µg of GSK583 or 100 µg of MDP were locally injected into the Ti + MDP group, the Ti + GSK583 group or the Ti + MDP + GSK583 group every day for 2 weeks.[22]

2.12 CT scan analysis and microcomputed tomography

After the calvaria were harvested, a 2-day formalin-fixation was followed by a scan with a high resolution in vivo micro-

CT imaging system (ZKKS-MCT-Sharp, Japan) using the qualitative analysis in the associated software. The radiographic projections were acquired at 60 kV and 667 μA within 240 ms. All projection frames were recorded five times and then averaged. 3D images were reconstructed using the associated manufacturer's reconstruction software. The bone mineral density, total volume, bone volume, BV/TV and porosity were measured from a 1 mm × 3 mm × 3 mm region of interest in cross-section slices around the sagittal suture.

2.13 Immunohistochemistry assay of mice calvaria

Mice calvaria were decalcified in 10% ethylene diamine tetra acetic acid (EDTA) for 21 days. Thereafter, the samples were fixed in 4% formalin fixation and then embedded in paraffin blocks for 4.0 μm serial sectioning. The sections were then dehydrated using ethanol washes of increasing concentration, and deparaffinized using xylene. Endogenous biotin or enzymes were blocked with 3% hydrogen peroxide, and antigen retrieval was treated with sodium citrate. Anti-mouse TRAP monoclonal antibodies (1 : 100 diluted, Abcam, USA), anti-mouse TNF-α monoclonal antibodies (1 : 100 diluted, Abcam, USA) and anti-mouse RANKL monoclonal antibodies (1 : 100 diluted, Abcam, USA) were used as primary antibodies, and EnVision Detection Systems (DAKO, Denmark) were used as secondary antibodies. The tissues were incubated at 37 °C for 1 hour with primary antibodies, respectively, then washed with phosphate buffered saline (PBS) 3 times, and incubated at 37 °C for 0.5 hours with secondary antibodies. DAB was used as a chromogenic agent, and hematoxylin was used for the second stain. Finally, the samples were washed with water, dried, and mounted with neutral balsam, then observed by a biomicroscope (DM2000, Leica, German). TRAP cell numbers were counted within an interested area. The interested area was defined using a magnification of 10×, as one microscope sight of the calvarial bone with the midline suture centered.[23] Osteoclasts were identified as large multinucleated cells located on the bone perimeter within resorption lacunae.

2.14 Statistics

All data *in vitro* were analyzed using the SPSS 20.0 software package (Chicago, IL, USA). Every result came from at least three independent experiments. Analysis of variance (ANOVA) for factorial design was used to analyze the interaction between NOD2-siRNA transfection or infection effects and particle stimulation effects. Repeated measures of ANOVA were used to analyze the difference between cell transfection and infection effects. One-way ANOVA with the Student–Newman–Keuls *post hoc t*-test was used to analyze the TNF-α production and the CT measurement of calvaria. Data were expressed as mean ± SD. $P < 0.05$ was considered as statistically significant.

3. Results

3.1 NOD2 and TNF-α were highly expressed in synovial membrane around the prosthesis in the aseptic loosening patients

A brown color represented the staining intensity of NOD2, TNF-α and RANKL expressed in cytoplasm. NOD2 and TNF-α were highly expressed in the synovial membrane around the prosthesis in the aseptic loosening patients. However, NOD2 and TNF-α were barely detected in patients with FHN. The staining intensity of RANKL was found to be moderate in both aseptic loosening and FHN patients (Fig. 1A). As for the immunoreactivity score for each group, the average IS of NOD2 in aseptic loosening patients was 1.67 ± 0.12, significantly higher than that in FHN patients (0.15 ± 0.13, $p < 0.01$). The same tendency was found in TNF-α, with an average IS of 2.05 ± 0.21 in aseptic loosening patients and 0.26 ± 0.12 in FHN patients ($p < 0.01$). The RANKL immunoreactivity score in FHN patients (1.83 ± 0.19) was slightly but significantly higher than that in aseptic loosening patients (1.13 ± 0.25, $p < 0.05$) (Fig. 1B).

3.2 The expressions of NOD2 and proinflammatory factors were up-regulated in RAW264.7 after stimulation

To investigate the expression of NOD2 and proinflammatory factors, we performed real-time PCR, western blotting, ELISA and immunofluorescent staining with the titanium particle stimulated macrophages RAW264.7. The mRNA expressions of NOD2 in the macrophages were significantly up-regulated after the stimulation by titanium particles at each time point ($p < 0.05$). Meanwhile, the mRNA expressions of TNF-α, iNOS, and COX2 were significantly higher at each time point ($p < 0.05$) (Fig. 2A). ELISA showed a similar result: the secreted proteins of TNF-α were significantly increased at every time point after stimulation ($p < 0.05$) (Fig. 2B). Immunofluorescence showed the increased expression of TNF-α around the macrophage after stimulation (Fig. 2C). Transcription factor signal transducer and activator of transcription 1 (STAT1) was also observed translocating into the cell nucleus after stimulation (Fig. 2D). Moreover, the protein expression of protein-38 (p38), phosphorylated protein-38 (p-p38), phosphorylated c-Jun N-terminal kinase (p-JNK), phosphorylated extracellular signal-regulated kinase (p-ERK), phosphorylated IκB kinase β (p-IKKβ) and p-STAT1 were up-regulated after stimulation in western blotting, indicating the activation of the MAPK pathways and NF-κB pathways, while the expression of JNK, ERK and STAT1 were not significantly increased after stimulation (Fig. 2E).

3.3 The higher expression of NOD2 and proinflammatory factors was observed in NOD2-knockdown lentivirus transfected RAW264.7 compared with the normal RAW264.7 after stimulation

NOD2-689 and NOD2-2920 yielded the greatest knockdown efficiency, with a down-regulation of 66–70% mRNA expression
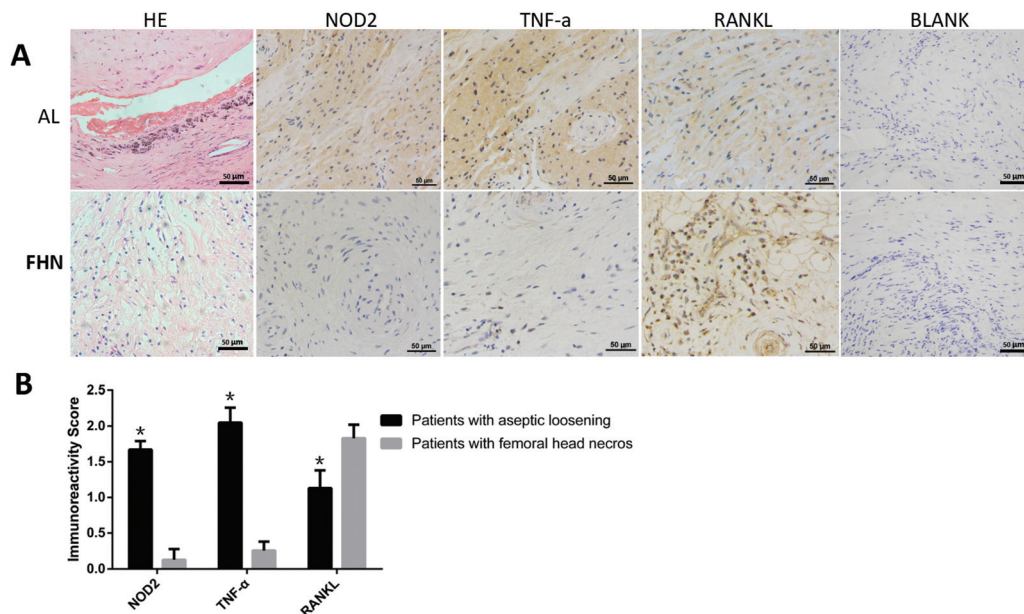
Fig. 1 The expression of NOD2, RANKL and TNF-α in the synovial membrane around the prosthesis in the aseptic loosening compared with FHN patients (AL: aseptic loosening). (A) The immunohistochemical staining of NOD2, RANKL HE and TNF-α from AL and FHN patients' hip synovial membrane. (B) The immunoreactivity score of NOD2, RANKL and TNF-α from AL and FHN patients' hip synovial membrane. *: Significant difference compared with FHN patients: $p < 0.05$.
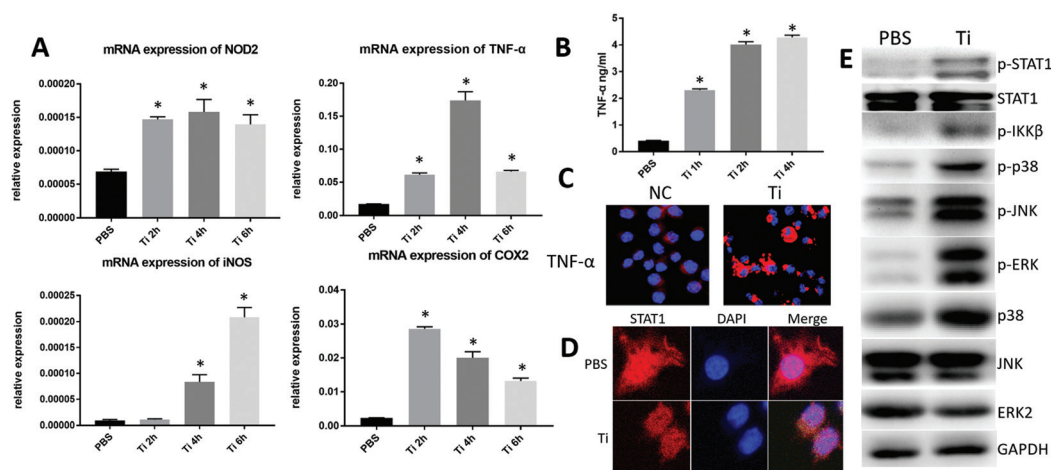

Fig. 2 The expression of NOD2, TNF-α, iNOS, COX2, STAT1, MAPK pathway and IKKβ in RAW264.7 after stimulation. (A) The mRNA expressions of NOD2, TNF-α, iNOS, COX2 in macrophages were significantly higher than the negative control after the stimulation by titanium particles at every time point ($p < 0.05$). (B) Secreted proteins of TNF-α were significantly increased at every time point after stimulation (1 h: 2.32 ± 0.06 ng ml^{-1}, 2 h: 4.01 ± 0.11 ng ml^{-1}, 4 h: 4.30 ± 0.07 ng ml^{-1} vs. 0 h: 0.41 ± 0.03 ng ml^{-1}, $p < 0.05$). (C) Expression of TNF-α in RAW264.7 after stimulation through an immunofluorescent scope. (D) STAT1 was observed to have translocated into the cell nucleus after stimulation. (E) The protein expression of STAT1, MAPK pathway and IKKβ in RAW264.7 after stimulation. *: $p < 0.05$.

and lowered protein expression (Fig. 3A and B). Recombinant lentivirus was then synthesized using the same sequence of NOD2-689 and NOD2-2920 siRNA respectively with a tag of green fluorescent protein (GFP). The FACS method was used to separate the transfected cells. The efficiency of the lentivirus for NOD2-shRNA transfection was 42–45% using flow cytometry. The infected cells were then selected by fluorescent cell sorting.

We then stimulated the transfected macrophage RAW264.7 with the titanium particles, and performed real-time PCR, western blotting, ELISA and immunofluorescent staining to examine the expression of proinflammatory factors. The figures show the results from the sequence of NOD2-689. An increased mRNA expression of TNF-α, IL-1β, iNOS and COX2 was observed in those transfected cells, compared with the
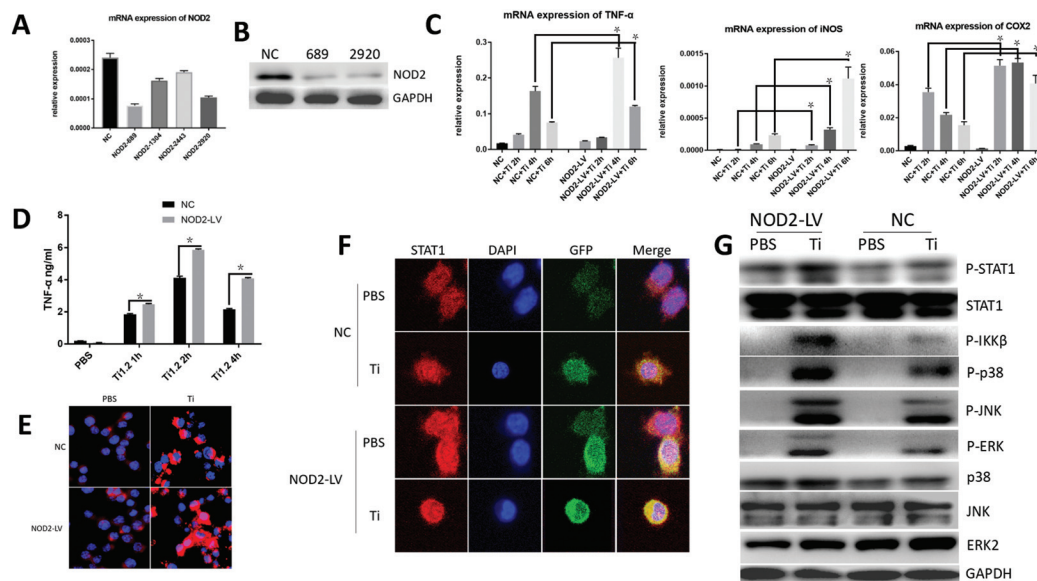
Fig. 3 The expression of TNF-α, STAT1, MAPK pathway and IKKβ in NOD2-knockdown lentivirus transfected RAW264.7 after stimulation. (A) The efficiencies of four siRNA sequences were assessed by PCR. (B) The efficiency of the two sequences NOD2-689 and NOD2-2920 yielding the most inhibition were assessed by western blotting. (C) The mRNA expression of NOD2, TNF-α, iNOS and COX2 in transfected RAW264.7 were higher than in normal cells at each time point after stimulation (*: $p < 0.05$). (D) More secreted TNF-α protein was detected in transfected RAW264.7 at every time point after stimulation (*: $p < 0.05$). (E) Higher expression of TNF-α in transfected RAW264.7 after stimulation. (F) STAT1 was observed to have translocated into the cell nucleus in transfected cells more than in normal cells after stimulation. (G) The protein expression of STAT1, MAPK pathway and IKKβ in transfected RAW264.7 was higher than in normal cells after stimulation.

normal macrophages after stimulation ($p < 0.05$) (Fig. 3C). ELISA showed a similar increase in the secreted proteins of TNF-α in transfected cells compared with normal cells after stimulation ($p < 0.05$) (Fig. 3D). The increase was also shown through immunofluorescence in the expression of TNF-α around the transfected cells compared with normal cells after stimulation (Fig. 3E). STAT1 was also observed to have more translocation in the transfected cell nucleus than in normal cells after stimulation (Fig. 3F). In addition, western blotting showed that the protein expression of p-p38, p-JNK, p-ERK, p-IKKβ and p-STAT1 were likewise up-regulated after stimulation in transfected cells, but the expressions of p38, JNK ERK and STAT1 remained the same, representing the strengthened activation of MAPK pathways and NF-κB pathways (Fig. 3E).

3.4 M1 polarization was observed in titanium particle stimulated RAW264.7 *via* flow cytometry

Flow cytometry was used to examine the polarization of normal and transfected macrophages stimulated by titanium particles. Macrophage bio-markers iNOS (M1) and CD206 (M2) were analyzed by flow cytometry to evaluate the different phenotypes (Fig. 4A). The RAW264.7 stimulated by PBS as a negative control contained barely any iNOS-positive cells (M1, 0.15 ± 0.01%) and a low percentage of CD206-positive cells (M2, 4.61 ± 1.41%). The transfected macrophages contained a similar percentage of iNOS-positive cells (1.1 ± 0.17%) and CD206-positive cells (2.57 ± 0.35%). Increases in the percentage of iNOS-positive cells (17.04 ± 0.90%, $p < 0.05$) and

CD206-positive cells (15.15 ± 4.48%, $p < 0.05$) were both observed in titanium particle treated RAW264.7. A higher increase in the percentage of iNOS-positive cells (22.49 ± 0.20%, $p < 0.05$) was observed in titanium particle treated transfected macrophages. While no significant difference was observed in the percentage of CD206-positive cells (13.94 ± 2.34%, $p > 0.05$) between normal and transfected macrophages (Fig. 4B and C).

3.5 The local injection of NOD2-knockdown lentivirus exacerbated the osteolysis of mice crania *in vivo*

We generated a cranial osteolysis mouse model, and the lentivirus carrying the sequence of NOD2-knockdown mentioned previously was also injected with the titanium particles. After harvesting the crania, micro-CT was performed to quantify the bone volume/tissue volume (BV/TV), porosity, and bone mineral density (BMD) of a 1 mm × 3 mm region of interest (ROI) around the cranial suture. A 3-dimensional reconstruction of the mice crania showed an area of osteolysis around the cranial sutures in the titanium particle treated mice. The local injection of lentivirus showed an exacerbated osteolysis around the cranial sutures. While both kinds of lentivirus injected mice crania showed no osteolysis, samples injected with titanium particles and NC lentivirus showed a similar level of osteolysis to the titanium particle group (Fig. 5A). Qualitative analysis showed a 15.0% decrease in BV/TV ($p < 0.05$) and a 56.1% decrease in BMD ($p < 0.05$) in the Ti + NOD2-LV group compared with the Ti group, while no significant difference was observed between the Ti + NC-LV group
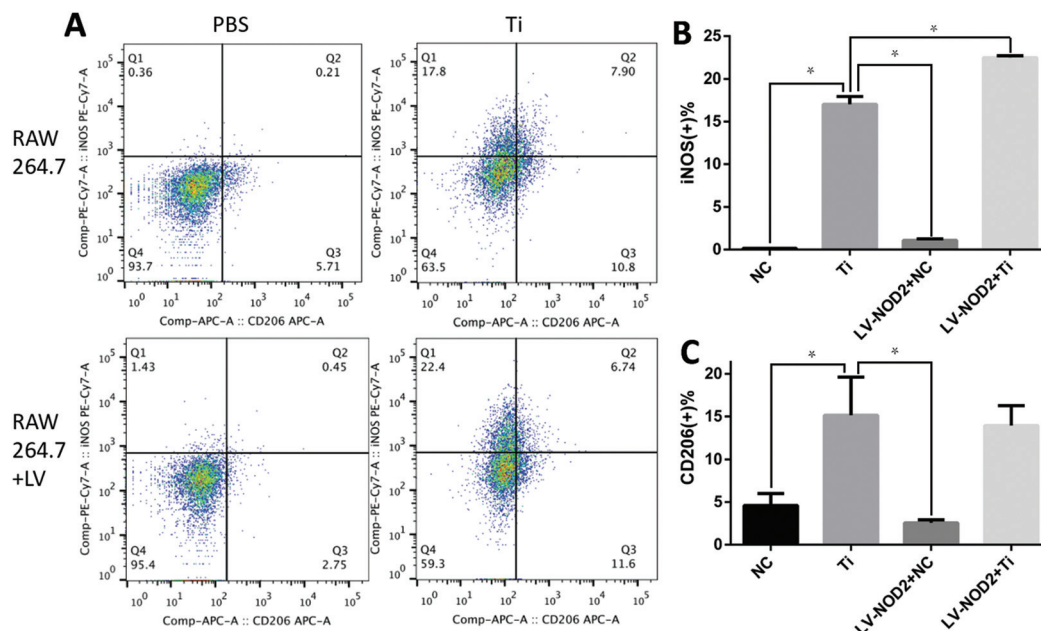
Fig. 4 Flow cytometry of macrophage polarization in lentivirus transfected RAW264.7 after stimulation. (A) Flow cytometry of macrophage polarization in lentivirus transfected RAW264.7 after stimulation. (B) Percentage of cells with positive iNOS in different treatments of RAW264.7 (*: $p < 0.05$). (C) Percentage of cells with positive CD206 in different treatments of RAW264.7 (*: $p < 0.05$).
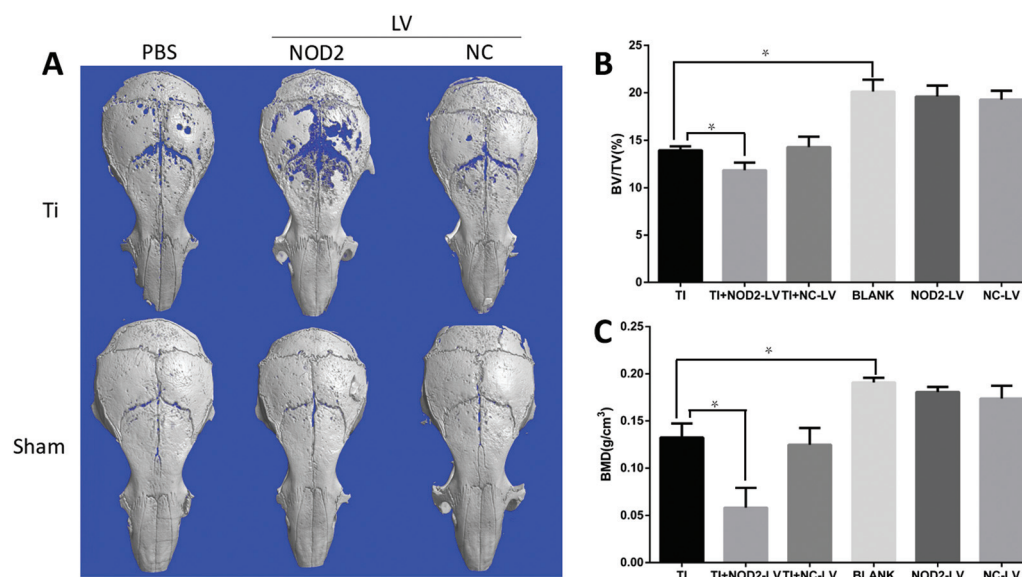

Fig. 5 Local injection of NOD2-knockdown lentivirus exacerbated the osteolysis of mice cranial *in vivo*. (A) A 3-dimensional reconstruction of the mice crania in different treatment groups. (B) The BV/TV of a 1 mm × 3 mm region of interest (ROI) around the cranial suture, with a 15.0% decrease in the Ti + NOD2-LV group compared with the Ti group (*: $p < 0.05$). (C) The BMD of a 1 mm × 3 mm ROI around the cranial suture, with a 56.1% decrease in the Ti + NOD2-LV group compared with the Ti group (*: $p < 0.05$).

and the Ti group in terms of BV/TV ($p > 0.05$) or BMD ($p > 0.05$)(Fig. 5B and C). BV/TV and BMD in the three non-titanium groups were all significantly higher than that in the Ti group, but no difference was found among the blank group, the NOD2-LV group, or the NC-LV group.

An immunohistochemistry assay of mice calvaria showed similar results. TNF-α and RANKL were found to be highly expressed in the calvaria from the Ti group, and even more highly in the NOD2-LV + TI group (Fig. 6A). TRAP cell numbers in the interested area showed a 105% increase in the Ti group and a 146% increase in the NOD2-LV + TI group compared with the blank group ($p < 0.05$), but no significant difference was found between the Ti group and the NOD2-LV + TI group ($p > 0.05$) (Fig. 6B).
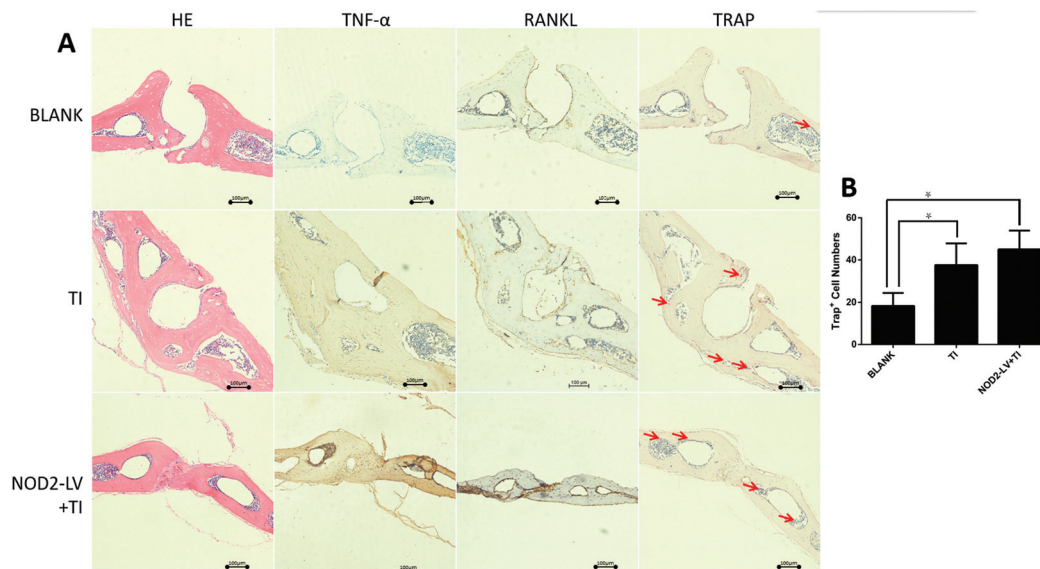
Fig. 6 The expression of TRAP, RANKL and TNF-α of mice calvaria sutura in different treatment groups. (A) The immunohistochemical staining of TRAP, RANKL and TNF-α of mice calvaria sutura in different treatment groups. TNF-α and RANKL were found to be highly expressed in the calvaria from the Ti group, and even more highly in the NOD2-LV + TI group. (B) TRAP cell numbers in the interested area showed a 105% increase in the Ti group and a 146% increase in the NOD2-LV + TI group compared with the blank group ($p < 0.05$), but no significant difference was found between the Ti group and the NOD2-LV + TI group ($p > 0.05$).

3.6 The enhancement of the expression of proinflammatory factor caused by MDP was inhibited by GSK583 *in vitro* and *in vivo*

To further investigate the contribution of NOD2 to the secretion of proinflammatory factors *in vitro*, we performed real-time PCR and ELISA with the RAW264.7 macrophages with treatment by titanium particles, MDP and GSK583. The mRNA expression of TNF-α and IL-1β in the MDP + Ti treated macrophages was significantly higher than that in the titanium treated macrophages ($p < 0.05$), while the MDP treatment could hardly induce the expression of TNF-α or IL-1β. Anyway, the augmentation of the proinflammatory factors expression in MDP + Ti treatment was inhibited by GSK583 in the MDP + Ti + GSK583 treated macrophages ($p < 0.05$), returning to the same proinflammatory factor expression level as the titanium treated macrophages ($p > 0.05$). Last but not least, the treatment with GSK583 did not down-regulate the titanium particle induced proinflammatory factor secretion (Fig. 7D). ELISA showed a similar result: titanium particle induced secretion of TNF-α was significantly increased when treated with MDP, and did not decrease after treatment with GSK583 ($p < 0.05$) (Fig. 7E).

To further investigate the contribution of NOD2 in particle induced peri-prosthesis osteolysis *in vivo*, a cranial osteolysis mouse model was generated, as mentioned previously. 40 µg of GSK583 or 100 µg of MDP were locally injected every day to maintain the drug concentration. The mice crania were harvested after a 2-week intervention, and then the BV/TV, porosity, and BMD of the injection area were measured. A 3D reconstruction of the mice crania showed an exacerbated osteolysis in the Ti + MDP group compared with the Ti group. Anyway,

samples of the TI + MDP + GSK583 group and the TI + GSK583 group showed a similar level of osteolysis to the TI group (Fig. 7A). Qualitative analysis showed an 11.1% decrease in the Ti + MDP group compared with the Ti group in terms of BV/TV ($p < 0.05$) and a 38.9% decrease in BMD ($p < 0.05$), while a 15.6% increase in the Ti + MDP + GSK583 group and a 15.5% increase in the Ti + GSK583 group were observed when compared with the Ti group in terms of BV/TV ($p < 0.05$). But no significant difference was found in BMD between the Ti group, the Ti + MDP + GSK583 group or the Ti + GSK583 group (Fig. 7B and C).

3.7 The establishment of the CRISPR-Cas9 NOD2 gene knockout mice and the enhancement of the mice calvarial osteolysis

A CRISPR-Cas9 NOD2 gene knockout mouse model was established in C57BL/6J mice to examine the contribution of NOD2. The NOD2-KO mice with a deletion of 47 bp (Chr8 88660549–88660595) was determined by direct gene sequencing (Fig. 8D). Moreover, the protein expression of NOD2 was suppressed in NOD2-KO mice tails, compared with the wild-type mice (Fig. 8E). A 3D pictorial illustration of the micro-CT scan indicated that NOD2-KO mice had an enhancement in cranial osteolysis (Fig. 8A). Qualitative analysis showed that no significant difference was found between NOD2-KO mice and WT mice in terms of BV/TV ($p > 0.05$) in the titanium particle treatment groups and blank groups ($p > 0.05$) (Fig. 8B). But the BMD of NOD2-KO mice was 53.1% lower than in the WT mice ($p < 0.05$) in the titanium particle treatment groups.
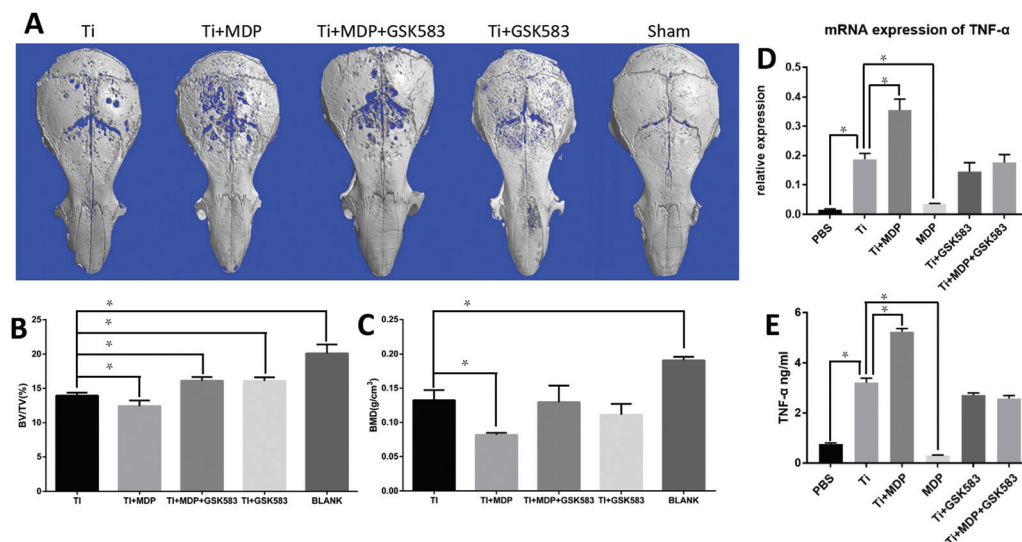
Fig. 7 The effect of MDP and GSK583 in cranial osteolysis mice model *in vivo* and in TNF-α expression from different titanium particle treated RAW264.7. (A) A 3D reconstruction of the mice crania in different treatment groups. (B and C) BV/TV and BMD of a 1 mm × 3 mm ROI around the cranial suture in different treatment groups. (D and E) TNF-α mRNA and secreted TNF-α expression in different treatment groups after stimulation. Titanium particle induced TNF-α and cranial osteolysis were significantly increased when treated with MDP, but did not decrease after treatment with GSK583 ($p < 0.05$).
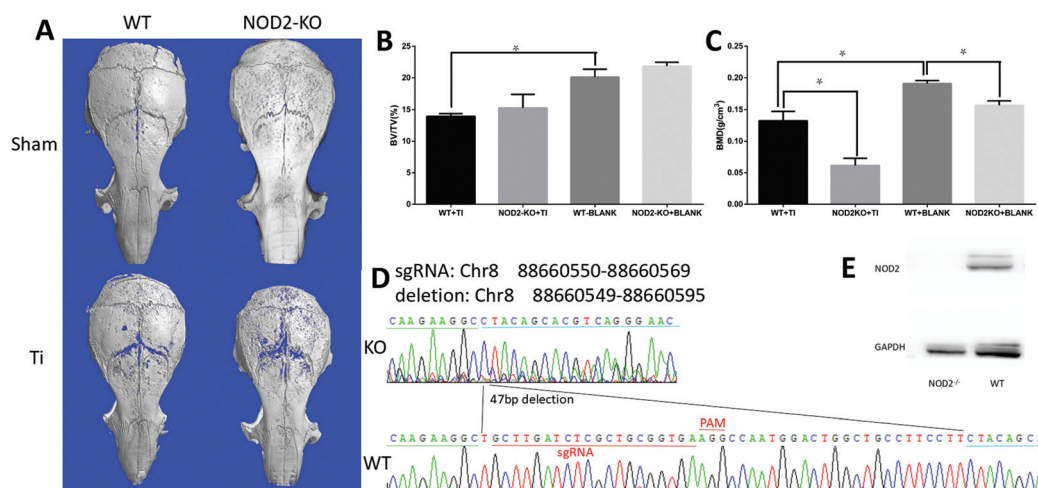

Fig. 8 The establishment of the CRISPR-Cas9 NOD2 gene knockout mice and the enhancement in the mice calvarial osteolysis. (A) 3D reconstruction of the mice crania in WT and CRISPR-Cas9 NOD2-KO mice. (B and C) BV/TV and BMD of a 1 mm × 3 mm ROI around the cranial suture in different treatment groups. (D) The direct gene sequencing of mice tails showed sgRNA and the deletion of 47 bp (Chr8 88660549−88660595). (E) Protein expression of NOD2 in NOD2-KO mice tails showed a suppressed NOD2 protein expression.

Meanwhile, the BMD of NOD2-KO mice was also 18.8% lower than for the WT mice ($p < 0.05$) in the blank groups (Fig. 8C).

4.　Discussion

Aseptic loosening has been proven to be the most common etiology of the long-term failure of prostheses in many clinical studies.[1–3] With the regeneration of prosthetic materials, their biotoxicity, biocompatibility and mechanical characteristics have been thoroughly improved due to the hard work and devotion of generations of researchers, but the chronic inflammation caused by wear particles still remains unsolved.[24] Nearly all kinds of the most popular prosthetic materials nowadays have been proved to produce wear particles which activate the immune system and finally cause aseptic loosening.[4] Even though materials like ceramics and highly cross-linked polyethylene (HXLPE) have been widely used to reduce the wear of prostheses, it is still vital to clarify the mechanism of aseptic loosening.

In our previous studies, types and sizes were defined as the most important factors for the biological characteristics of wear particles. A larger biological effect was caused by smaller wear particles.[7,8] What is more, titanium particles were proved to induce greater secretion of proinflammatory cytokines than ceramic of the same volume and diameter; however, the immune-reaction, the activation of the TLR pathway, was the same.[7] Thus, titanium particles ranging from 0.2 µm to 1.2 µm were chosen in this study to stimulate the maximal biological effect. In our recent study, NLRs had been found to be highly expressed in the synovial membrane samples from aseptic loosening patients, just like TLR2 and TLR4.[9] A large number of studies had focused on TLR2, TLR4 and even NLRP3 in different cells and different wear particles. But few studies had reported the role of NOD2 in aseptic loosening.

NOD2, an intracellular receptor of MDP derived from bacteria, provides a secondary defensive line for cells by contributing to the maintenance of cell homeostasis and the induction of immune inflammation.[14] NOD2 is normally held in an auto-inhibited state by its LRRs and NACHT domains. When activated by peptidoglycan fragments, NOD2 binds nucleotides and oligomerizes through NACHT domains and initiates the downstream signalling molecule RIP2 through CARD domains.[25] NOD2 was proved to participate in different kinds of bacterial infections such as *Acinetobacter baumannii*, and other immune system diseases such as Crohn's disease.[14,26] In this study, NOD2 and TNF-α were observed to be simultaneously highly expressed in the synovial membrane around the prosthesis in aseptic loosening patients. What is more, the mRNA and protein expression of NOD2 was up-regulated in RAW264.7 after stimulation by titanium particles and was similar to the up-regulation of proinflammatory factors and inflammation pathways such as the MAPK pathway and the NF-κB pathway. These results strongly indicated that NOD2 was involved in the process of wear particle induced immunoreaction. The expression of RANKL should both be up-regulated in aseptic loosening patients and in the calvaria from the Ti group, as a reflection of osteoclast activation, but FHN did not provide an ideal negative control. We consider the expression of RANKL not to be decreased in aseptic loosening patients, but to be increased in FHN patients instead. The higher expression of RANKL in FHN patients was reported in cartilage,[27] indicating that there might be some other mechanisms for the up-regulation of RANKL in FHN patients. More research is required into FHN.

At the beginning, as a member of PRRs, NOD2 was hypothesized to be another receptor that recognizes titanium particles and initiates inflammation pathways. In order to clarify the role of NOD2, we generated the NOD2-knockdown lentivirus transfected macrophage RAW264.7. Surprisingly, the mRNA expressions of TNF-α, IL-1β, iNOS and COX2 were raised. In the meantime, protein expressions of the MAPK pathway and the NF-κB pathway were also up-regulated. The increase was also shown through immunofluorescence in the higher expression of TNF-α around the transfected cells than around normal cells after stimulation. STAT1 was also observed with more translocation in the transfected cell nucleus than in normal cells after stimulation. These results indicated that NOD2 might play a negative role in titanium particle induced immunoreaction.

In recent years, a concept of M1 and M2 macrophages in macrophage polarization has been established.[28] M1 polarization is induced by inflammation signalling and then responds with cell-mediated immunity, including effective antigen presentation and the production of proinflammatory cytokines and chemokines.[29,30] M2 macrophage activation was mainly caused by cytokines IL-4 or IL-13. This kind of polarization is achieved by suppression of proinflammatory cytokine production, and finally produces anti-inflammatory mediators and a distinct set of chemokines.[28] It has been proved that a macrophage will switch into M1 polarization when stimulated by titanium particles.[6] The same results were shown in our study: the percentage of M1 polarization macrophage was increased. What is more, when stimulated by titanium particles, the NOD2-knockdown macrophage ended up with a larger percentage of M1 polarization macrophage compared to normal cells. These results further proved that NOD2 might play a negative role in titanium particle induced immunoreaction. Interestingly, Ti significantly promoted both iNOS + (M1 type) and CD206 + (M2 type) macrophages in our research, and similar results were observed in some other research.[6,31] The up-regulation of M2 macrophage percentages might be a feedback response for M1 polarization and the secretion the massive proinflammatory cytokine. In any case, the exact mechanism requires more exploratory work.

To redouble the evidence for the negative effect from NOD2, we generated a cranial osteolysis mouse model. To make sure that the titanium particles keep stimulating the interested area for 2 weeks, a gelatin sponge was used to maintain the suspension of titanium particles and allow them to be released slowly. Micro-CT was used to identify tiny differences and to quantify the osteolysis effects. Like the results *in vitro*, the local injection of NOD2-knockdown lentivirus exacerbated the osteolysis of crania, with a lower BV/TV and a significantly lower BMD. An immunohistochemistry assay of mice calvaria showed similar results. TNF-α and RANKL were observed to be more highly expressed in the lentivirus injection mice. Anyway, neither the efficiency of the transfection nor the distribution of lentivirus could be observed or quantified after the injection. More work is still required to clarify the usage of the local injection of lentivirus in the cranial osteolysis mice mode.

To come to definite conclusions about whether or not NOD2 played a negative role in titanium particle induced immunoreaction *in vivo*, we generated a CRISPR-Cas9 NOD2 gene knockout mice mode. The RNA-guided CRISPR-Cas nuclease system is guided by small RNAs that pair with target DNA, and are markedly easier to design, highly specific, and efficient for a variety of cell types and organisms.[32] We chose and synthesized three sgRNA to minimize the off-target mutagenesis. The NOD2-KO mice we used in this study contain a deletion of 47 bp (Chr8 88660549–88660595)

according to direct gene sequencing. Then we performed the cranial osteolysis mice mode on these NOD2-KO mice. Qualitative analysis showed that no significant difference was found between NOD2-KO mice and WT mice in terms of BV/TV, with or without stimulation. But the BMD of NOD2-KO mice was significantly lower than of WT mice in titanium particle treatment groups. Meanwhile, the BMD of NOD2-KO mice was also slightly but significantly lower than that of WT mice in the blank groups. Because of the time spent on direct gene sequencing, we performed the mice cranial osteolysis surgery at the age of 25 weeks. Thus, the lower BMD in NOD2-KO mice without stimulation may be mainly due to their elderly age. Anyway, the NOD2-KO mice suffered a greater BMD decrease (60.5% vs. 31.9%), indicating a similar conclusion for a negative role of NOD2.

Up to now, we have demonstrated that NOD2, one of the PRRs, has played a negative role in the titanium particle induced immunoreaction, but the mechanism remains unclear. Also it is unclear how NOD2 down-regulated the immunoreaction not by itself but through any downstream molecules. In recent times, NOD2 had been reported to interact with and be suppressed by TLR2/4 in intestinal epithelial cells.[33] Also NOD2 was reported to suppress colorectal tumorigenesis via down-regulating the TLR pathways, by induction of IRF4.[34] Yet none of the articles shed light upon the mechanism of NOD2's down-regulation effect.

On activation by MDP, NOD2 undergoes self-oligomerization and recruitment of the downstream adaptor molecule, RIPK2, via homophilic CARD–CARD interaction.[16] Active RIPK2 leads to the activation of NF-κB pathways, which translocates it to the nucleus and starts the transcription of the proinflammatory gene. Or it activates MAP kinases and transcription factor activator protein 1 involved in cell proliferation, differentiation. RIPK2 is essential for most of NOD2's functions.[14] Therefore, we chose a potent, selective, and bioavailable RIPK2 inhibitor, GSK583,[20] to cut down the effect of the NOD2/RIPK2 correlated pathways. The mRNA expression of the proinflammatory factor in MDP + Ti treated macrophages was significantly higher than those titanium treated macrophages, but the augmentation of the proinflammatory factor expression was inhibited by GSK583, returning to the same level as titanium treated macrophages. What is more, the treatment of GSK583 did not down-regulate the titanium particle induced proinflammatory factor secretion. Similar results were observed in ELISA and the cranial osteolysis mouse model. These results indicated that the pathways associated with RIPK2 were not involved in the titanium particle induced immunoreaction.

TLR2 and TLR4 are widely known as the most important PRRs in recognizing wear particles. Therefore, if NOD2 interacts with and down-regulate TLR2 and TLR4, when it is knocked down, the TLR2 and TLR4 pathways will be excessively activated, and affect all the downstream pathways, including the MAPK pathways and NF-κB pathways, ending up with excessively expressed proinflammatory factors and excessive osteolysis.

5. Conclusions

In conclusion, our study demonstrated that NOD2 plays a negative role in osteolysis induced by titanium particles both *in vitro* and *in vivo*, but not as a PRR.

Conflicts of interest

The authors declare no conflict of interest.

Acknowledgements

References

1 M. Porter, M. Boroff, P. Gregg, A. MacGregor, P. Howard, C. Esler, A. John, M. Porteus, A. Carr, J. Pelan, R. Beaumont, J. Thornton, M. Wright, E. Young, O. Forsyth, A. Mistry, C. Newell, M. Pickford, M. Royal and A. Goldberg OBE, The UK National Joint Registry Annual Report 2013, Technical Report, 2014.

2 H. Maradit Kremers, D. R. Larson, C. S. Crowson, W. K. Kremers, R. E. Washington, C. A. Steiner, W. A. Jiranek and D. J. Berry, Prevalence of Total Hip and Knee Replacement in the United States, *J. Bone Jt. Surg., Am. Vol.*, 2015, **97**(17), 1386–1397.

3 American Joint Replacement Registry (AJRR) 2018 Annual Report. 2018, AAOS.

4 M. Takagi, Y. Takakubo, J. Pajarinen, Y. Naganuma, H. Oki, M. Maruyama and S. B. Goodman, Danger of frustrated sensors: Role of Toll-like receptors and NOD-like receptors in aseptic and septic inflammations around total hip replacements, *J. Orthop. Transl.*, 2017, **10**, 68–85.

5 S. Grosse, H. K. Haugland, P. Lilleng, P. Ellison, G. Hallan and P. J. Hol, Wear particles and ions from cemented and uncemented titanium-based hip prostheses-a histological and chemical analysis of retrieval material, *J. Biomed. Mater. Res., Part B*, 2015, **103**(3), 709–717.

6 J. Pajarinen, V. Kouri, E. Jämsen, T. Li, J. Mandelin and Y. T. Konttinen, The response of macrophages to titanium particles is determined by macrophage polarization, *Acta Biomater.*, 2013, **9**(11), 9229–9240.

7 Y. Ding, C. Q. Qin, Y. R. Fu, J. Xu and D. S. Huang, In vitro comparison of the biological activity of alumina ceramic and titanium particles associated with aseptic loosening, *Biomed. Mater.*, 2012, 7(4), 45019.

8 C. Zhang, C. Li, S. Li, L. Qin, M. Luo, G. Fu, J. Qiu, P. Peng, W. Cai and Y. Ding, Small Heterodimer Partner Negatively Regulates TLR4 Signaling Pathway of Titanium Particles-Induced Osteolysis in Mice, *J. Biomed. Nanotechnol.*, 2018, 14(3), 609–618.

9 K. Manyuan, L. I. Shixun, T. Jianshao, L. I. Changchuan, F. U. Guangtao, Q. Junxiong, P. Peng and D. Yue, Expression and related research of NODs in periprosthetic tissue of aseptic hip joint loosening, *China Sciencepap.*, 2018, 13(12), 1329–1335.

10 Z. Ceng, Y. Ding, J. Xu, J. Huang, C. Qin, S. Wen and B. Barden, The expression of Toll-like receptors 2 and 4 in the macrophages of hip synovium, *Chin. J. Clin. Anat.*, 2011, 29(05), 557–560.

11 O. Takeuchi and S. Akira, Pattern Recognition Receptors and Inflammation, *Cell*, 2010, 140(6), 805–820.

12 L. Samelko, S. Landgraeber, K. McAllister, J. Jacobs and N. J. Hallab, TLR4 (not TLR2) dominate cognate TLR activity associated with CoCrMo implant particles, *J. Orthop. Res.*, 2017, 35(5), 1007–1017.

13 D. Rachmawati, H. J. Bontkes, M. I. Verstege, J. Muris, B. M. von Blomberg, R. J. Scheper and I. M. van Hoogstraten, Transition metal sensing by Toll-like receptor-4: next to nickel, cobalt and palladium are potent human dendritic cell stimulators, *Contact Dermatitis*, 2013, 68(6), 331–338.

14 A. Negroni, M. Pierdomenico, S. Cucchiara and L. Stronati, NOD2 and inflammation: current insights, *J. Inflammation Res.*, 2018, (11), 49–60.

15 I. Tattoli, L. A. Carneiro, M. Jéhanno, J. G. Magalhaes, Y. Shu, D. J. Philpott, D. Arnoult and S. E. Girardin, NLRX1 is a mitochondrial NOD-like receptor that amplifies NF-κB and JNK pathways by inducing reactive oxygen species production, *EMBO Rep.*, 2008, 9(3), 293–300.

16 C. B. Moore, D. T. Bergstralh, J. A. Duncan, Y. Lei, T. E. Morrison, A. G. Zimmermann, M. A. Accavitti-Loper, V. J. Madden, L. Sun, Z. Ye, J. D. Lich, M. T. Heise, Z. Chen and J. P. Ting, NLRX1 is a regulator of mitochondrial antiviral immunity, *Nature*, 2008, 451(7178), 573–577.

17 R. S. Bresalier, S. B. Ho, H. L. Schoeppner, Y. S. Kim, M. H. Sleisenger, P. Brodt and J. C. Byrd, Enhanced sialylation of mucin-associated carbohydrate structures in human colon cancer metastasis, *Gastroenterology*, 1996, 110(5), 1354–1367.

18 R. E. Unger, K. Peters, A. Sartoris, C. Freese and C. J. Kirkpatrick, Human endothelial cell-based assay for endotoxin as sensitive as the conventional Limulus Amebocyte Lysate assay, *Biomaterials*, 2014, 35(10), 3180–3187.

19 H. Tang, U. Amara, D. Tang, M. A. Barnes, C. McDonald and L. E. Nagy, Synergistic interaction between C5a and NOD2 signaling in the regulation of chemokine expression in RAW 264.7 macrophages, *Adv. Biosci. Biotechnol.*, 2013, 4(8C), 30–37.

20 X. He, R. S. Da, J. Nelson, X. Zhu, T. Jiang, B. Okram, S. Jiang, P. Y. Michellys, M. Iskandar, S. Espinola, Y. Jia, B. Bursulaya, A. Kreusch, M. Y. Gao, G. Spraggon, J. Baaten, L. Clemmer, S. Meeusen, D. Huang, R. Hill, V. Nguyen-Tran, J. Fathman, B. Liu, T. Tuntland, P. Gordon, T. Hollenbeck, K. Ng, J. Shi, L. Bordone and H. Liu, Identification of Potent and Selective RIPK2 Inhibitors for the Treatment of Inflammatory Diseases, *ACS Med. Chem. Lett.*, 2017, 8(10), 1048–1053.

21 W. H. Tsai, D. Y. Huang, Y. H. Yu, C. Y. Chen and W. W. Lin, Dual roles of NOD2 in TLR4-mediated signal transduction and -induced inflammatory gene expression in macrophages, *Cell. Microbiol.*, 2011, 13(5), 717–730.

22 M. Ishida, H. Kitaura, K. Kimura, H. Sugisawa, T. Aonuma, H. Takada and T. Takano-Yamamoto, Muramyl dipeptide enhances lipopolysaccharide-induced osteoclast formation and bone resorption through increased RANKL expression in stromal cells, *J. Immunol. Res.*, 2015, 2015, 132765.

23 M. von Knoch, D. E. Jewison, J. D. Sibonga, R. T. Turner, B. F. Morrey, F. Loer, D. J. Berry and S. P. Scully, Decrease in particle-induced osteolysis in obese (ob/ob) mice, *Biomaterials*, 2004, 25(19), 4675–4681.

24 P. Sadoghi, M. Liebensteiner, M. Agreiter, A. Leithner, N. Bohler and G. Labek, Revision surgery after total joint arthroplasty: a complication-based analysis using worldwide arthroplasty registers, *J. Arthroplasty*, 2013, 28(8), 1329–1332.

25 D. Corridoni and A. Simmons, Innate immune receptors for cross-presentation: The expanding role of NLRs, *Mol. Immunol.*, 2017, DOI: 10.1016/j.molimm.2017.11.028.

26 S. D. Kale, N. Dikshit, P. Kumar, V. Balamuralidhar, H. J. Khameneh, N. Bin Abdul Malik, T. H. Koh, G. G. Y. Tan, T. T. Tan, A. Mortellaro and B. Sukumaran, Nod2 is required for the early innate immune clearance of Acinetobacter baumannii from the lungs, *Sci. Rep.*, 2017, 7(1), 17429.

27 X. Qin, P. Jin, T. Jiang, M. Li, J. Tan, H. Wu, L. Zheng and J. Zhao, A Human Chondrocyte-Derived In Vitro Model of Alcohol-Induced and Steroid-Induced Femoral Head Necrosis, *Med. Sci. Monit.*, 2018, 24, 539–547.

28 S. Gordon and P. R. Taylor, Monocyte and macrophage heterogeneity, *Nat. Rev. Immunol.*, 2005, 5(12), 953–964.

29 Q. Gu, H. Yang and Q. Shi, Macrophages and bone inflammation, *J. Orthop. Transl.*, 2017, 10, 86–93.

30 J. Ma, T. Chen, J. Mandelin, A. Ceponis, N. E. Miller, M. Hukkanen, G. F. Ma and Y. T. Konttinen, Regulation of macrophage activation, *Cell. Mol. Life Sci.*, 2003, 60(11), 2334–2346.

31 B. Li, Y. Hu, Y. Zhao, M. Cheng, H. Qin, T. Cheng, Q. Wang, X. Peng and X. Zhang, Curcumin Attenuates Titanium Particle-Induced Inflammation by Regulating Macrophage Polarization In Vitro and In Vivo, *Front. Immunol.*, 2017, 8, 55.

32 L. Cong and F. Zhang, Genome engineering using CRISPR-Cas9 system, *Methods Mol. Biol.*, 2015, **1239**, 197–217.

33 E. Layunta, E. Latorre, R. Forcen, L. Grasa, M. Castro, M. A. Arias, A. I. Alcalde and J. E. Mesonero, NOD2 Modulates Serotonin Transporter and Interacts with TLR2 and TLR4 in Intestinal Epithelial Cells, *Cell. Physiol. Biochem.*, 2018, **47**(3), 1217–1229.

34 S. Udden, L. Peng, J. L. Gan, J. M. Shelton, J. S. Malter, L. V. Hooper and M. H. Zaki, NOD2 Suppresses Colorectal Tumorigenesis via Downregulation of the TLR Pathways, *Cell Rep.*, 2017, **19**(13), 2756–2770.